Published in final edited form as:
Bioconjug Chem. 2012 September 19; 23(9): 1775–1782. doi:10.1021/bc200696b.

Synthesis and Preclinical Evaluation of Bifunctional Ligands for Improved Chelation Chemistry of ^{90}Y and ^{177}Lu for Targeted Radioimmunotherapy

Chi Soo Kang[1], **Xiang Sun**[1], **Fang Jia**[2], **Hyun A Song**[1], **Yunwei Chen**[1], **Michael Lewis**[2], and **Hyun-Soon Chong**[1,*]

[1]Chemistry Division, Biological and Chemical Sciences Department, Illinois Institute of Technology, Chicago, IL

[2]Department of Veterinary Medicine and Surgery, Department of Radiology, Nuclear Science and Engineering Institute, University of Missouri-Columbia, Columbia, MO

Abstract

We report a practical and high yield synthesis of a bimodal bifunctional ligand 3p-*C*-NETA-NCS containing the isothiocyanate group for conjugation to a tumor targeting antibody. 3p-*C*-NETA-NCS was conjugated to a tumor-targeting antibody, trastuzumab, and the corresponding 3p-*C*-NETA-trastuzumab conjugate was evaluated and compared to trastuzumab conjugates of the known bifunctional ligands *C*-DOTA, *C*-DTPA, *C*-NOTA, and 3p-*C*-DEPA for radiolabeling kinetics with ^{90}Y and ^{177}Lu. 3p-*C*-NETA-trastuzumab conjugate exhibited extremely rapid complexation kinetics with ^{90}Y and ^{177}Lu. ^{90}Y-3p-*C*-NETA-trastuzumab and ^{177}Lu-3p-*C*-NETA-trastuzumab conjugates were stable in human serum for 2 weeks. A pilot biodistribution study was conducted to evaluate *in vivo* stability and tumor targeting of ^{177}Lu-radiolabeled trastuzumab conjugate using nude mice bearing ZR-75-1 human breast cancer. ^{177}Lu-3p-*C*-NETA-trastuzumab conjugate displayed low radioactivity level at blood (1.6%), low organ uptake (<2.2%), and high tumor-to-blood ratio (6.4) at 120 h. 3p-*C*-NETA possesses favorable *in vitro* and *in vivo* profiles and is an excellent bifunctional chelator that can be used for targeted RIT applications using ^{90}Y and ^{177}Lu and has potential to replace DOTA and DTPA analogues in current clinical use.

Introduction

Radioimmunotherapy (RIT) is a potent therapeutic technique applicable to numerous cancers.[1–2] Two RIT drugs, Zevalin® and Bexxar® are clinically available for treatment of B-cell non-Hodgkin's lymphoma (NHL).[3–5] The RIT system generally consists of three components, a radionuclide, a tumor-targeting antibody or peptide, and a bifunctional ligand.[2,6] β-emitting radionuclides, ^{90}Y and ^{177}Lu have been extensively explored for RIT. Highly energetic ^{90}Y ($t_{1/2}$ = 64.1 h, E_{max} = 2.3 MeV) has the advantage of a relatively long-range tissue penetration and homogeneous dose distribution.[2,6] Less energetic ^{177}Lu ($t_{1/2}$ = 6.7 d, E_{max} = 0.5 MeV) has a shorter penetration range relative to ^{90}Y and is proposed to provide more selective tumor targeting and resultant lower normal tissue damage and better tolerance by patients.[2] Its longer half-life is sufficient for preparation and shipment of radioimmunoconjugate and allows for maximal delivery of dose to tumors.[2]

*To whom correspondence should be addressed. Chong@iit.edu, Phone: 312-567-3235, Fax: 312-567-3494. Mailing address: 3101 S. Dearborn St, LS 182, Chemistry Division, Biological and Chemical Sciences Department, Illinois Institute of Technology, Chicago, IL, 60616.

Supporting material. HPLC and ITLC chromatograms for assessment of radiolabeling reaction kinetics and serum stability and *in vivo* biodistribution data. This material is available free of charge via the Internet at http://pubs.acs.org/BC.

C-DOTA (Figure 1) forms a stable complex with lanthanides including ^{90}Y and ^{177}Lu.[7–8] The enhanced stability of the metal complexes of DOTA compared to acyclic ligand such as *C*-DTPA (Figure 1) is attributed to the macrocyclic effect and increased pre-organization.[9,10] The therapeutic efficacy of ^{90}Y- or ^{177}Lu-labeled DOTA-antibody conjugates has been demonstrated in preclinical and clinical trials.[2,11,12] However, the slow formation kinetics and low radiolabeling efficiency of *C*-DOTA in binding ^{90}Y and ^{177}Lu remains a limitation in broad RIT applications of the macrocyclic chelate.[12–13] Rapid radiolabeling kinetics of a bifunctional ligand conjugated to an antibody is required to minimize radiolytic damage to protein conjugates that can occur during radiolabeling of an antibody conjugate with high specific activity for therapeutic applications.[14] Development of superior chelation chemistry that allows for scale-up production of stable ^{90}Y- or ^{177}Lu-radiolabeled radioimmunoconjugates under mild and practical radiolabeling conditions is necessary for effective and safe RIT applications of ^{90}Y and ^{177}Lu. We have synthesized the bimodal ligands in the series of NETA and DEPA (Figure 1) that possess both macrocyclic and acyclic moieties for cooperative metal binding.[15–18] The acyclic pendant donor groups in NETA or DEPA are proposed to rapidly initiate coordination to the metal, as in the case of DTPA, while the macrocyclic component, a partial NOTA or DOTA backbone, is expected to tightly wrap around the metal ion trapped by the acyclic binding groups and thereby achieve maximum complex stability by saturating the metal coordination sphere. The NETA- and DEPA-backboned chelators were shown to display favorable complexation kinetics and stability in binding ^{90}Y, ^{177}Lu, or $^{205/6}$Bi.[15–18]

Herein, we report an efficient synthesis of bifunctional ligand 3p-*C*-NETA-NCS containing the isothiocyanate group for conjugation to a tumor targeting antibody. 3p-*C*-NETA-NCS conjugated to trastuzumab was compared to trastuzumab conjugates of the known bifunctional ligands *C*-DOTA, *C*-DTPA, and 3p-*C*-DEPA for radiolabeling kinetics with ^{90}Y and ^{177}Lu. ^{90}Y-and ^{177}Lu-radiolabeled trastuzumab conjugates of 3p-*C*-NETA, 3p-*C*-DEPA, and *C*-DOTA were evaluated for *in vitro* serum stability. ^{177}Lu-3p-*C*-NETA-trastuzumab conjugate was also evaluated for *in vivo* biodistribution and tumor uptake study.

Experimental Procedure

Instruments and methods

^{1}H, ^{13}C, and DEPT NMR spectra were obtained using a Bruker 300 instrument and chemical shifts are reported in ppm on the δ scale relative to TMS. Electro spray ionization (ESI) high resolution mass spectra (HRMS) were obtained on JEOL double sector JMS-AX505HA mass spectrometer (University of Notre Dame, IN). Size-exclusion HPLC (SE-HPLC) chromatograms were obtained on Agilent 1200 equipped with a diode array detector and an in-line IN/US γ-Ram Model 2 radiodetector (Tampa, FL) fitted with Bio-Silect SEC 250-5 column (Bio-Rad, Hercules, CA), TSK-G3000PW column (Tosoh bioscience, King of Prussia, PA), or a BioSep-SEC S 3000 column (Phenomenex, Torrance, CA).

Reagents

All reagents were purchased from Sigma-Aldrich (St. Louis, MO) and used as received unless otherwise noted. Trastuzumab (Herceptin; Genentech, South San Francisco, CA) was obtained through the Veterinary Resources Program (National Institutes of Health, Bethesda, MD) and provided by Dr. Martin Brechbiel (Radioimmune and Inorganic Chemistry Section, Radiation Oncology Branch, NIH). ^{90}Y (0.05M HCl) and ^{177}Lu (0.05M HCl) were purchased from Perkin Elmer. *C*-DOTA was purchased from Macrocyclics (Dallas, TX).

Caution: ^{90}Y ($t_{1/2}$ = 64.1 h) is a β-emitting radionuclide. ^{177}Lu ($t_{1/2}$ = 6.7 days) is a β/γ-emitting radionuclide. Appropriate shielding and handling protocols should be in place when using the isotope.

tert-butyl 2-{[2-(tert-butoxy)-2-oxoethyl][2-iodo-5-(4-nitrophenyl)pentyl]amino} acetate (3)

To a solution of **1**[18] (100 mg, 0.221 mmol) and PPh_3 (69.5 mg, 0.265 mmol) in CH_2Cl_2 (2 mL) at 0 °C was added imidazole (18 mg, 0.265 mmol) and iodine (67.3 mg, 0.265 mmol) portionwise over 5 min. The reaction mixture was stirred for 4 h at 0 °C and RT for 1 h after which the reaction mixture was concentrated to dryness. The residue was purified by silica gel (60–230 mesh) column chromatography eluted with 10% ethyl acetate in hexanes to afford **3** (120 mg, 97%) as a brownish oil. ^1H NMR ($CDCl_3$, 300 MHz) δ 1.45 (s, 18H), 1.71–1.82 (m, 2H), 1.83–2.05 (m, 2H), 2.66–2.87 (m, 2H), 2.90–3.01 (m, 1H), 3.23–3.36 (m, 1H), 3.36–3.50 (m, 4H), 4.10–4.18 (m, 1H), 7.35 (d, J = 8.6 Hz, 2H), 8.14 (d, J = 8.6 Hz, 2H); ^{13}C NMR ($CDCl_3$, 300 MHz) δ 28.2 (q), 30.8 (t), 34.9 (t), 36.0 (d), 36.3 (t), 56.9 (t), 64.1 (t), 81.2 (s), 123.6 (d), 129.2 (d), 146.4 (s), 149.9 (s), 170.4 (s). HRMS (Positive ion FAB) Calcd for $C_{23}H_{36}IN_2O_6$: $[M - I + OH]^+$ *m/z* 453.2601. Found: $[M - I + OH]^+$ *m/z* 453.2603.

tert-butyl-2-[(1-{4,7-bis[2-(tert-butoxy)-2-oxoethyl]-1,4,7-triazonan-1-yl}-5-[4-(hydroxyl-nitro)phenyl]pentan-2-yl)[2-(tert-butoxy)-2-oxoethyl]amino]acetate (7)—

To a solution of **3** (50 mg, 0.089 mmol) in CH_3CN (1 mL) at 0 °C was added compound **5** (35.0 mg, 0.098 mmol) and DIPEA (34.5 mg, 0.267 mmol). The resulting mixture was stirred for 40 h at room temperature, while monitoring the reaction progress using TLC. The reaction mixture was concentrated to dryness. The residue was purified via column chromatography on silica gel (220–440 mesh) eluting with 3% CH_3OH in CH_2Cl_2 to provide product **7** (65 mg, 94%). ^1H and ^{13}C NMR data of **7** were identical to those as previously reported.[18]

tert-butyl-2-[(1-{4,7-bis[2-(tert-butoxy)-2-oxoethyl]-1,4,7-triazonan-1-yl}-5-[4-(hydroxyl-nitro)phenyl]pentan-2-yl)[2-(tert-butoxy)-2-oxoethyl]amino]acetate (7)

Reaction of 2 with 5 in the presence of $AgClO_4$: To a solution of **2** (50 mg, 0.097 mmol) in CH_3CN (0.5 mL) at −5 °C was added $AgClO_4$ (20.1 mg, 0.097 mmol) and stirred for 10 min at the same temperature. Then, compound **5** (34.7 mg, 0.097 mmol) and DIPEA (37.6 mg, 0.291 mmol) in CH_3CN (0.5 mL) was sequentially added to the reaction mixture at −5 °C. The resulting mixture was warmed to room temperature and stirred for 24 h while monitoring the reaction progress using TLC. The residue was purified via column chromatography on silica gel (60–230 mesh) eluting with 3% CH_3OH in CH_2Cl_2 to provide the crude product **7** containing a tiny amount of the starting material **5** as an impurity. The crude product was treated with 0.1M HCl solution (10 mL) and extracted with $CHCl_3$ (10 mL × 3). The combined organic layers were concentrated to dryness. The residue was treated with 0.1M NaOH solution (10 mL) and extracted with $CHCl_3$ (10 mL × 3). The combined organic layers were dried over $MgSO_4$, filtered, and concentrated *in vacuo* to the dryness to provide product **7** (66 mg, 86%) as a yellowish oil. ^1H and ^{13}C NMR data of **7** were identical to those as previously reported.[18]

tert-butyl-2-[(1-{4,7-bis[2-(tert-butoxy)-2-oxoethyl]-1,4,7-triazonan-1-yl}-5-[4-(hydroxyl-nitro)phenyl]pentan-2-yl)[2-(tert-butoxy)-2-oxoethyl]amino]acetate (7)

Reaction of 3 with 5 in the presence of $AgClO_4$: To a solution of **3** (50 mg, 0.089 mmol) in CH_3CN (0.5 mL) at −5 °C was added $AgClO_4$ (18.4 mg, 0.089 mmol) and stirred for 10

min at the same temperature. Then, compound **5** (31.8 mg, 0.089 mmol) and DIPEA (34.5 mg, 0.267 mmol) in CH_3CN (0.5 mL) was sequentially added to the reaction mixture at −5 °C. The resulting mixture was warmed to room temperature and stirred for 24 h while monitoring the reaction progress using TLC. The residue was purified via column chromatography on silica gel (60–230 mesh) eluting with 3% CH_3OH in CH_2Cl_2 to provide the crude product **7** containing a tiny amount of the starting material **5** as an impurity. The crude product was treated with 0.1M HCl solution (10 mL) and extracted with $CHCl_3$ (10 mL × 3). The combined organic layers were concentrated to dryness. The residue was treated with 0.1M NaOH solution (10 mL) and extracted with $CHCl_3$ (10 mL × 3). The combined organic layers were dried over $MgSO_4$, filtered, and concentrated *in vacuo* to the dryness to provide product **7** (62 mg, 88%) as a yellowish oil. ^1H and ^{13}C NMR data of **7** were identical to those as previously reported.[18]

{4-[5-(4-Aminophenyl)-2-(bis-*tert*-butoxycarbonylmethylamino) pentyl]-7-*tert*-butoxycarbo-nylmethyl-[1,4,7]triazonan-1-yl} acetic acid *tert*-butyl ester (8)— To a solution of **7** (14.6 mg, 0.018 mmol) in ethanol (5 mL) at room temperature was added 10% Pd/C (3 mg) under Ar (g). The reaction mixture was placed under hydrogenation apparatus for 14 h. The resulting mixture was filtered via celite bed and washed thoroughly with ethanol. The filtrate was concentrated to provide **8** (13.1 mg, 93%) as a yellowish solid. ^1H NMR ($CDCl_3$, 300 MHz) δ 1.35–1.70 (m, 40H), 1.92–2.05 (m, 1H), 2.18–2.32 (m, 1H), 2.38–2.90 (m, 15H), 3.08 (d, J = 16.6 Hz, 1H), 3.26 (d, J = 16.5 Hz, 1H), 3.34 (s, 2H), 3.44 (s, 4H), 6.60 (d, J = 8.3 Hz, 2H), 6.94 (d, J = 8.2 Hz, 2H); ^{13}C NMR ($CDCl_3$, 300 MHz) δ 27.8(t), 28.0(q), 28.1(t), 28.4(t), 29.6(t), 35.8(t), 51.3(t), 51.7(t), 53.5(t), 54.7(t), 55.9(t), 58.1(t), 58.5(t), 59.4(d), 81.2(s), 81.3(s), 82.2(s), 115.2(d), 119.1(d), 131.2(s), 145.5(s), 170.7(s), 170.9(s), 171.4(s). HRMS (Positive ion FAB) Calcd for $C_{41}H_{72}N_5O_8$: $[M + H]^+$ *m/z* 762.5381. Found: $[M + H]^+$ *m/z* 762.5364.

{4-[5-(4-Amino-phenyl)-2-(bis-carboxymethylamino)pentyl]-7-carboxymethyl-[1,4,7]triazo-nan-1-yl}acetic acid (9)—To a flask containing compound **8** (8.5 mg, 0.011 mmol) at 0 – 5 °C was added dropwise 4M HCl (g) in 1,4-dioxane (3 mL) over 20 min. The resulting mixture was gradually warmed to room temperature and continuously stirred for 18 h. Ether (20 mL) was added to the reaction mixture which was then stirred for 10 min. The resulting mixture was placed in the freezer for 1 h. The resulting precipitate was filtered and washed with ether. The solid product was quickly dissolved in deionized water. The aqueous solution was concentrated *in vacuo* to provide **9** (7.1 mg, 88%) as an off-white solid. ^1H NMR (D_2O, 300 MHz) δ 1.50–1.73 (m, 4H), 2.53–2.65 (m, 2H), 3.00–3.35 (m, 10H), 3.49–3.85 (m, 13H), 7.17–7.30 (m, 4H); ^{13}C NMR (D_2O, 300 MHz) δ 25.7 (t), 26.6 (t), 33.5 (t), 48.2 (t), 49.6 (t), 50.4 (t), 51.8 (t), 52.5 (t), 53.7 (t), 54.0 (t), 56.0 (t), 60.3 (d), 123.0 (d), 127.5 (s), 130.0 (d), 142.2 (s), 168.0 (s), 170.0 (s), 173.6 (s). HRMS (Positive ion FAB) Calcd for $C_{25}H_{40}N_5O_8$: $[M + H]^+$ *m/z* 538.2877. Found: $[M + H]^+$ *m/z* 538.2880.

{4-[2-(Bis-carboxymethylamino)-5-(4-isothiocyanatophenyl) pentyl]-7-carboxymethyl[1,4,7] triazonan-1-yl}acetic acid (3p-*C*-NETA-NCS, 10)—To a solution of **9** (6.3 mg, 0.009 mmol) in water (0.15 mL) was added dropwise 1M thiophosgene in $CHCl_3$ (11 μL, 0.011 mmol). The resulting mixture was stirred at room temperature for 3 h. The aqueous layer was concentrated *in vacuo* to provide pure **10** (6.0 mg, 95%) as a light yellowish solid. ^1H NMR (D_2O, 300 MHz) δ 1.50–1.75 (m, 4H), 2.50–2.61 (m, 2H), 2.95–4.02 (m, 23H), 7.13 (s, 4H). HRMS (Positive ion FAB) Calcd for $C_{26}H_{38}N_5O_8S$: $[M + H]^+$ *m/z* 580.2441. Found: $[M + H]^+$ *m/z* 580.2439.

Conjugation of 3p-*C*-NETA-NCS to trastuzumab: *C*-DTPA-NCS, 3p-*C*-DEPA-NCS, and *C*-DOTA-NCS were conjugated to trastuzumab as previously reported.[16] All absorbance

measurements were obtained on an Agilent 8453 diode array spectrophotometer equipped with a 8-cell transport system (designed for 1 cm cells). Metal-free stock solutions of all buffers were prepared using Chelex®-100 resin (200–400 mesh, Bio-Rad Lab, Hercules, CA, Cat# 142-2842). Chelex resin (1 g/100 mL) was added into the buffer solution and the mixture was shaken overnight in a shaker and filtered through a Corning filter system (Cat# 430513, pore size 0.2 μm). Disposable PD-10 Sephadex™ G-25M columns (GE Healthcare, #17-0851-01) were rinsed with 25 mL of the conjugation buffer prior to addition of antibody. Amicon centricon C-50 (50,000 MWCO) centrifugal filter devices (Millipore, Cat# UFC805008) were used for purification of trastuzumab conjugate (Bedford, MA). The initial concentration of trastuzumab was determined by UV/Vis spectroscopic method. Phosphate buffered saline (PBS, 1×, 11.9 mM Phosphates, 137 mM NaCl, and 2.7 mM KCl, pH 7.4) was purchased from Fisher and used as received. Conjugation buffer (50 mM HEPES, 150 mM NaCl, pH 8.6) was prepared as 1× solutions, chelexed, and filtered through the Corning filter. Trastuzumab (9.2 mg) was diluted to 2.5 mL using conjugation buffer and the resulting solution was added to a PD-10 column. Conjugation buffer (6.0 mL) was added to the PD-10 column to exchange the buffer solution of the antibody and collected in a sterile test tube and checked for the presence of trastuzumab via analysis of the UV/VIS spectrum at 280 nm. To a sterile test tube containing the recovered trastuzumab (7.0 mg) was added a 10-fold excess of 3p-*C*-NETA-NCS (45 μL, 10 mM). The resulting solution was gently agitated for 16 h at room temperature and placed on a Centricon C-50 membrane and spun down to reduce volume. PBS (3 × 2 mL) was added to the remaining solution of the 3p-*C*-NETA-trastuzumab conjugate followed by centrifugation to remove unreacted ligand. The volume of purified conjugate antibody was brought to 1.0 mL. To measure [trastuzumab] in the conjugates, a UV/Vis spectrometer was zeroed against a cuvette filled with 2 mL of PBS with a window open from 190 nm to 1100 nm. A 50 μL portion of PBS was removed and discarded, 50 μl of the 3p-*C*-NETA-trastuzumab conjugate solution was added, and absorbance of the solution at 280 nm was noted. Beer's Law was used to calculate [trastuzumab] in the conjugate with molar absorptivity of 1.42. After centrifugation, 5.9 mg (4.06×10^{-5} M, 84%) of the trastuzumab remained.

Spectroscopic Determination of Ligand to Protein (L/P) Ratio

A stock solution of the Lu(III)-AAIII reagent was prepared in 0.15 M NH_4OAc (pH 7.0) by adding an aliquot of lutetium atomic absorption solution (5.79×10^{-3} M) into a 10 μM solution of AAIII to afford a 5 μM solution of Lu(III). This solution was stored in the dark to avoid degradation over time. A UV/Vis spectrometer was zeroed against well-dried 8 blank cuvettes with a window open from 190 nm to 1100 nm. A cuvette was filled with AAIII solution (2 mL), and the other seven cuvettes with the Lu(III)-AAIII (2 mL). Lu(III)-AAIII (50 μL) in the seven cuvettes was removed and discarded. Milli-Q water (50 μL) was added to the second cuvette, and one to five 10 μL additions of 3p-*C*-NETA (0.1 mM) were added to the five cuvettes to give a series of five different concentrations (2 mL total volume). The solutions in the third to the seventh cuvette were diluted to 2.0 mL by adding an aliquot of milli-Q water. Trastuzumab conjugate of 3p-*C*-NETA (50 μL) was added to the eighth cuvette containing Lu(III)-AAIII reagent (1950 μL). After addition of trastuzumab conjugate to the Lu(III)-AAIII solution, the resulting solution was equilibrated for 10 min. The absorbance of the resulting solution at 652 nm was monitored every 30 seconds over 6 min. The average of the absorbance of each solution was calculated, and the absorbance data from the Lu(III)-AAIII solution containing six different concentrations were used to construct a calibration plot of A_{652} versus [3p-*C*-NETA] by the equation, $Y = 0.1202-(1.2138 \times 10^4)$[3p-*C*-NETA] ($R^2 = 0.9967$) wherein $Y = A_{652nm}$. The concentration of 3p-*C*-NETA in the trastuzumab conjugate was calculated (1.27×10^{-4}). The L/P ratio of 3p-*C*-NETA-trastuzumab conjugate ([1.27×10^{-4} M]/[4.06×10^{-5} M]) was measured to be 3.1.

Radiolabeling of bifunctional ligand-trastuzumab conjugates with ^{90}Y or ^{177}Lu

C-DTPA-trastuzumab, 3p-*C*-DEPA-trastuzumab, and *C*-DOTA-trastuzumab conjugates were prepared and purified as previously reported.[16] All HCl solutions were prepared from ultra-pure HCl (Fisher, Cat# A466-500). For metal-free radiolabeling, plasticware including pipette tips, tubes, and caps was soaked in 0.1M HCl overnight, washed thoroughly with Milli-Q (18.2 M3) water, and air-dried overnight. Ultra pure NH_4OAc (Aldrich, #372331) was purchased from Aldrich and used to prepare all NH_4OAc buffer solutions (0.25 M, pH 5.5). The buffer solutions were treated with Chelex-100 resin (Biorad, #142-2842, 1g/100 ml buffer solution), shaken overnight at room temperature, and filtered through 0.22 μm filter (Corning, #430320) prior to use. To a buffer solution (30 μL, pH 5.5) in a capped microcentrifuge tube (1.5 mL, Fisher Scientific #05-408-129) was sequentially added a solution of bifunctional ligand-trastuzumab conjugate (30 μg) in PBS (5~10 μL) and ^{177}Lu (0.05 M HCl, 60 μCi, 2~3 μL). To a conjugate solution (15~27 μL, 30 μg) in a capped microcentrifuge tube (1.5 mL) was sequentially added a solution of 0.05 M HCl (6~15 μL) and ^{90}Y (0.05 M HCl, 60 μCi, 2~4 μL). The final volume of the resulting solution was around 40 μL, and the pH of the resulting reaction mixture was 5.5. The reaction mixture was agitated on the thermomixer (Eppendorf, #022670549) set at 1,000 rpm at room temperature for 1 h. The labeling efficiency was determined by SE-HPLC (Bio-Silect SEC 250-5 column, PBS (pH 7.4) at a flow rate of 1ml/min for method 1; BioSep-SEC S 3000, a solution of 0.05M $NaSO_4$/0.02M NaH_2PO_4/0.05% NaN_3 (pH 6.8) at a flow rate of 1 ml/min for method 2; or TSK-G3000 PW column, PBS (pH 7.4) at a flow rate of 1 mL/min for method 3) and ITLC (solvent: 20mM EDTA/0.15M NH_4OAc).

A solution of radiolabeled mixture (6 μL) was withdrawn at the designated time points (1 min, 5 min, 10 min, 20 min, 30 min, and 60 min), and DTPA solution (10mM, 0.6 μL) was added to the mixture, and the resulting mixture was left for at least 20 min at RT. In ITLC analysis, peaks for bound and unbound radioisotope appeared around 30 mm and 50 mm from the origin, respectively. Bound and unbound radioisotope peaks appeared around 7.8 min and 10.7 min (Method 1), 9.0 min and 12.0 min (method 2), and 6.5 min and 8.5 min (method 3), respectively.

In vitro stability of ^{90}Y- and ^{177}Lu-radiolabeled trastuzumab conjugate

The radiolabeled trastuzumab conjugates were evaluated for stability in human serum (pH 7, 37 °C). ^{177}Lu-3p-*C*-NETA-trastuzumab, ^{177}Lu-*C*-DOTA-trastuzumab, or ^{177}Lu-3p-*C*-DEPA-trastuzumab was radiolabeled with ^{177}Lu at RT or 37 °C (0.25 M NH_4OAc, pH 5.5). The complex formed was purified by gel filtration chromatography using Biospin 6 column (Biorad, Cat# 732-6002) eluted with PBS (pH 7.4). The fraction containing ^{177}Lu-3p-*C*-NETA-trastuzumab (150 μL, ~200 μCi), ^{177}Lu-*C*-DOTA-trastuzumab (30 μL, ~100 μCi) or ^{177}Lu-3p-*C*-DEPA-trastuzumab (30 μL, ~100 μCi) was added into human serum (1 mL, Gemini Bioproducts, #100110) in a microcentrifuge tube. The stability of the purified ^{177}Lu-3p-*C*-NETA-trastuzumab or ^{177}Lu-*C*-DOTA-trastuzumab in human serum (37 °C, pH 7) was evaluated for 14 days, and ^{177}Lu-3p-*C*-DEPA-trastuzumab in human serum (37 °C, pH 7) was evaluated for 2 days.

^{90}Y-3p-*C*-NETA-trastuzumab, ^{90}Y-*C*-DOTA-trastuzumab, or ^{90}Y-3p-*C*-DEPA-trastuzumab was radiolabeled with ^{90}Y at RT or 37 °C (0.25 M NH_4OAc, pH 5.5). The complex formed was purified by gel filtration chromatography using Biospin 6 column (Biospin 6 chromatography columns, Biorad, Cat# 732-6002) or PD-10 Sephadex™ G-25M columns (GE Healthcare, #17-0851-01) eluted with PBS (pH 7.4). The fraction containing ^{90}Y-3p-*C*-NETA-trastuzumab (20 μL, ~110 μCi), ^{90}Y-*C*-DOTA-trastuzumab (30 μL, ~110 μCi), or ^{90}Y-3p-*C*-DEPA-trastuzumab (560 μL, 128 μCi) was added into human serum (1 mL, Gemini Bioproducts, #100110) in a microcentrifuge tube. The stability of the

purified ^{90}Y-3p-*C*-NETA-trastuzumab or ^{90}Y-*C*-DOTA-trastuzumab in human serum (37 °C, pH 7) was evaluated for 14 days. The stability of ^{90}Y-3p-*C*-DEPA-trastuzumab in human serum (37 °C, pH 7) was evaluated for 7 days.

The serum stability of ^{90}Y- or ^{177}Lu-radiolabeled complex (37 °C, pH 7) was assessed by measuring the transfer of the radionuclide from the complex to serum proteins using SE-HPLC (BioSep-SEC S 3000 column at a flow rate of 1 mL/min, eluent: 0.05M $NaSO_4$/0.02M NaH_2PO_4/0.05% NaN_3, pH 6.8 for method 2 or TSK-G3000PW column at a flow rate of 1 ml/min, eluent: PBS for method 3). A solution of the radiolabeled complex in serum (1–100 μL) was withdrawn at the designated time point, treated with DTPA (10 mM, 1–10 μL or 5 mM, 0.6 μL), incubated at room temperature for 20 min and then diluted with the HPLC eluent (160–200 μL) prior to SE-HPLC.

Radiolabeling with ^{177}Lu of trastuzumab conjugate for *in vivo* studies

3p-*C*-NETA-trastuzumab was radiolabeled with ^{177}Lu for a trial biodistribution study. An aliquot of 0.25 M NH_4OAc (65.8 μL, pH = 5.0) was added to a solution of $^{177}LuCl_3$ (424 μCi, 2.3 μL) in 0.05 M HCl followed by 100 μg of 3p-*C*-NETA-trastuzumab in a solution of 0.25 M NH_4OAc (15.9 μL, pH = 7.0). The reaction mixture was incubated at room temperature for 15 min with mixing at 1000 rpm and quenched with 1mM diethylenetriaminepentaacetic acid (DTPA) solution (pH = 6.0). The reaction mixture was allowed to stand for 15 min at room temperature and then radiochemical purity and yield was determined using TLC (silica gel, Methanol:10% NH_4OAC = 1:1). The dose was then prepared for injection to mice without further purification.

Biodistribution study

All experiments were conducted in compliance with the guidelines established by the Animal Care and Use Committee of the University of Missouri-Columbia Animal Care Quality Assurance Office. Athymic nude mice were implanted subcutaneously (s.c.) in the hind flank with a suspension of 5×10^6 ZR-75-1 human breast cancer cells (0.15 mL) in Hank's Balanced Salt Solution. When tumors had grown to 100–400 mg (~30 days after tumor implantation), mice were injected intravenously (i.v.) via the tail vein with ^{177}Lu-3p-*C*-NETA-trastuzumab (27 μCi, 100 μL). The biodistributions were obtained at 24, 72, and 120 h post-injection. Tissues harvested included blood, liver, bone and tumor. Tissues were drained of blood, weighed, and counted in a gamma counter with a standard of the injected dose, such that decay-corrected uptakes were calculated as percent injected dose per gram of tissue (% ID/g) and percent injected dose per organ (% ID/organ).

Results and Discussion

The key step in the synthesis of 3p-*C*-NETA-NCS is the regiospecific ring opening reaction of *N,N*-bisubstituted aziridinium ions **4** or **6** by bisubstituted 1,4,7-triazacyclononane (**5**) to generate the key precursor molecule **7** (Schemes 1 and 2). We recently reported the construction of **7** from the reaction of *N,N*-bisubstituted secondary β-amino bromide **2** with **5** based on the ring opening strategy.[18] The intermediate compound **7** was efficiently prepared in 82% isolated yield, and no byproduct was formed during the ring opening reaction. However, the reaction was very slow at room temperature and remained incomplete after 5 days. The mild reaction condition was required because an elevated temperature promoted the formation of an unwanted byproduct from intramolecular rearrangement of **2**.[18]

Inspired by high efficiency and regiospecificity of the ring opening reaction of aziridinium ion, we sought optimization of the reaction conditions for the synthesis of **7**. We envisioned

using secondary β-amino iodide **3** as the starting material based on the rationale that **3** containing iodine as an excellent leaving group would react significantly faster with the nucleophilic TACN analogue **5** and can be converted to **7** in higher isolated yield. We also investigated the use of a halo-sequestering agent $AgClO_4$ to see if the prompt formation of the azridinium ion can facilitate the nucleophilic attack of **5**. The optimization results are outlined in Scheme 1. Secondary β-amino iodide **3** was prepared using the efficient synthetic method that we developed. Iodination of **1**[18] using I_2, imidazole, and PPh_3 provided **3** in 97% isolated yield. Formation of aziridinium salt **4** from intramolecular rearrangement of **3** and subsequent regiospecific ring opening of **4** by nucleophilic bisubstituted TACN **5** at the less hindered carbon provided the desired coupling product **7** in excellent isolated yield (94%). The effect of silver perchlorate on the formation of **7** was explored using secondary β-amino halides **2** and **3**.

Treatment of **2** or **3** with silver perchlorate provided aziridinium perchlorate salt **6** which was further treated with **5** to provide the product **7** in 86% and 88% isolated yield, respectively. Our optimization strategy to prepare the key precursor **7** in an improved yield and at a shorter reaction time was found to be successful. The best result was obtained from the reaction of the secondary β-amino iodide **3** with **5** in the absence of silver perchlorate. It is noteworthy that both of the silver-promoted ring opening reactions produced a small portion of the intramolecular rearrangement byproduct. Synthesis of the bifunctional ligand 3p-*C*-NETA-NCS (**10**) was accomplished as shown in Scheme 2. Compound **7** was hydrogenated using 10% Pd/C to afford compound **8** in 93% isolated yield. *tert*-butyl groups in **8** was removed by the treatment of **8** with 4M HCl (g) in 1,4-dioxane. Reaction of **9** with thiophosgene in $CHCl_3/H_2O$ provided the desired 3p-*C*-NETA-NCS. The synthesis of 3p-*C*-NETA-NCS was achieved in 71% overall yield starting from the readily available compound **1**. The efficient synthetic method to **7** can be readily scaled up and applied to preparation of many other bifunctional chelates.

Trastuzumab is known to target HER2 (Human Epidermal growth factor receptor 2) overproduced in cancer cells and is a clinically available antibody for treatment of metastatic breast cancer.[19–20] 3p-*C*-NETA-NCS was conjugated with trastuzumab, and concentration of trastuzumab in the conjugate was quantified by the spectroscopic assay.[16] Ligand to protein ratio (L/P = 3.1) of 3p-*C*-NETA-trastuzumab conjugate was determined using Lu(III)-ArsenazoIII based UV-Vis spectrophotometric assay.[16] Trastuzumab conjugates of other bifunctional ligands (*C*-DOTA, *C*-DTPA, and 3p-*C*-DEPA) were also prepared and evaluated for comparison. The purified trastuzumab conjugate (0.25M NH_4OAc, pH 5.5) was labeled with ^{90}Y or ^{177}Lu at room temperature (RT).[18] During the reaction time (1 h), the components were analyzed using SE-HPLC after challenging the reaction mixture with 10 mM DTPA, and the radiolabeling efficiency (%) was determined using both ITLC and size exclusion (SE)-HPLC (Tables 1 and 2 and Supporting Information). The radiolabeling formation kinetics data indicate that 3p-*C*-NETA-trastuzumab conjugates were extremely rapid in binding ^{90}Y and ^{177}Lu and complexation was nearly complete in 1 min as determined by ITLC (91.6% for ^{90}Y and 99.2% for ^{177}Lu). Complexation kinetics of 3p-*C*-NETA-trastuzumab conjugate with ^{90}Y and ^{177}Lu was comparable to that of *C*-DTPA-trastuzumab conjugate. *C*-DOTA-trastuzumab displayed significantly slower complexation kinetics with ^{90}Y (71.7% at 1 h, Table 1), while the conjugate more rapidly bound to ^{177}Lu (>90% at 30 min, Table 2). 3p-*C*-DEPA-trastuzumab conjugate exhibited similar ^{90}Y- and ^{177}Lu-radiolabeling pattern to *C*-DOTA-trastuzumab, achieving the respective radiolabeling efficiency of ~67% (1 h, Table 1) and >87% (30 min, Table 2) with ^{90}Y and ^{177}Lu. It appears that decadentate 3p-*C*-DEPA has too many donor groups to form a stable Y(III) or Lu(III) complex, and this may allow the formation of the Lu(III)- or Y(III)-3p-*C*-DEPA complex to be a reversible process. The results indicates that the tridentate pendant acyclic donors in 3p-*C*-NETA are essential in rapidly binding Y(III) and

Lu(III) and improved complexation kinetics of NETA with the metals relative to DOTA is ascribed to cooperative and bimodal binding of acyclic and macrocyclic donors.

^{90}Y- or ^{177}Lu-radiolabeled trastuzumab conjugates of 3p-*C*-NETA, 3p-*C*-DEPA, and *C*-DOTA were further evaluated for *in vitro* serum stability (Supporting Information). Both ^{90}Y-3p-*C*-NETA-trastuzumab and ^{177}Lu-3p-*C*-NETA-trastuzumab remained stable in human serum for 2 weeks as confirmed by radio-SE-HPLC analysis. However, significant amount of the radioactivity was dissociated from ^{90}Y-3p-*C*-DEPA-trastuzumab (32%, 2 days) and ^{177}Lu-3p-*C*-DEPA trastuzumab (45%, 2 days). ^{90}Y-*C*-DOTA-trastuzumab and ^{177}Lu-*C*-DOTA-trastuzumab were quite stable releasing a minimal level of the radioactivity over 2 weeks.

The *in vitro* result suggests that 3p-*C*-NETA was favorably compared to *C*-DOTA and displayed excellent complexation kinetics and stability with ^{90}Y and ^{177}Lu. 1B4M-DTPA[20] has been used as the chelator of ^{90}Y in Zevalin and was reported to exhibit rapid complexation kinetics with ^{90}Y. However, it should be noted that ^{90}Y-1B4M-DTPA-antibody conjugate was less stable than ^{90}Y-DOTA-antibody conjugate both *in vitro* and *in vivo*.[21]

The *in vivo* stability and tumor targeting of ^{177}Lu-3p-*C*-NETA–trastuzumab was evaluated by performing a pilot biodistribution study in ZR-75-1-bearing nude mice (Figure 2). The 3p-*C*-NETA-trastuzumab conjugate was radiolabeled with ^{177}Lu at specific activity of 640 Ci/mmol and in 92.2% yield and radiochemical purity. The highest tumor uptake (10.55 ± 7.93%) of ^{177}Lu-3p-*C*-NETA-trastuzumab was observed at 72 h. ^{177}Lu-3p-*C*-NETA–trastuzumab exhibited the highest radioactivity level in the blood at 24 h (14.57 ± 10.63%), which was not significantly different than 72 h (12.09 ± 1.12%), but significantly decreased at 120 h (1.58 ± 1.30%). The ^{177}Lu-3p-*C*-NETA-trastuzumab conjugate resulted in a very low radioactivity level in the liver (2.20 ± 0.06%) and the kidneys (1.09 ± 0.12%) at 120 h. The radioimmunoconjugate displayed low bone uptake and a higher radioactivity level in the tumor, compared to the normal organs, over the course of the study and the highest tumor-to-blood ratio (4.39) at 120 h. The biodistribution data indicate that ^{177}Lu-3p-*C*-NETA remains stable *in vivo* and tumor targeting of ^{177}Lu-3p-*C*-NETA–trastuzumab can be improved by selecting an adequate HER2-positive tumor model.

Conclusion

Highly efficient and scalable synthetic route to the new bimodal bifunctional ligand 3p-*C*-NETA centered on formation of *N,N*-bisubstituted β-amino iodide and nucleophilic ring opening of an aziridinium ion was developed. The bimodal ligands, 3p-*C*-NETA and 3p-*C*-DEPA and other known bifunctional ligands, *C*-DOTA, and *C*-DTPA were evaluated for comparative ^{90}Y and ^{177}Lu-radiolabeleing kinetics study. 3p-*C*-NETA-trastuzumab conjugate instantly bound to ^{90}Y or ^{177}Lu with comparable radiolabeling kinetics to *C*-DTPA-trastuzumab conjugate, while 3p-*C*-DEPA- and *C*-DOTA-trastuzumab conjugates displayed similar and slow radiolabeling pattern in binding ^{90}Y and ^{177}Lu. Both ^{90}Y-3p-*C*-NETA-trastuzumab and ^{177}Lu-3p-*C*-NETA-trastuzumab were stable in human serum over 2 weeks. Significant amount of the radioactivity was released from both ^{90}Y-3p-*C*-DEPA-trastuzumab and ^{177}Lu-3p-*C*-DEPA-trastuzumab in serum over 24 h. ^{177}Lu-3p-*C*-NETA-trastuzumab conjugate produced a favorable biodistribution profile and exhibited low radioactivity level in organs and high tumor uptake. The results of the *in vitro* and *in vivo* studies indicate that bimodal and cooperative binding of the acyclic and macrocyclic moieties property in 3p-*C*-NETA led to fast complexation kinetics and high complex stability of the octadentate chelate in binding the lanthanides Y(III) and Lu(III). The bimodal ligand 3p-*C*-NETA has broad applications for RIT of various cancers using ^{90}Y

and ^{177}Lu. Based on the favorable *in vitro* complexation and *in vivo* biodistribution data, 3p-*C*-NETA-NCS radiolabeled with ^{90}Y or ^{177}Lu will be further evaluated for comprehensive *in vivo* biodistribution, pharmacokinetics, and dosimetry using different antibodies and tumor models.

Supplementary Material

Refer to Web version on PubMed Central for supplementary material.

Acknowledgments

We acknowledge the financial support from the National Institutes of Health (R01CA112503 to H. S. Chong). We also acknowledge the Department of Veterans Affairs, for providing resources and use of facilities at the Harry S. Truman Memorial Veterans' Hospital in Columbia, MO.

References

1. Knox SJ, Meredith RF. Clinical radioimmunotherapy. Sem Radiat Oncol. 2000; 10:73–93.
2. Milenic DE, Brady ED, Brechbiel MW. Antibody-targeted radiation cancer therapy. Nature Rev. 2004; 3:488–98.
3. Wiseman GA, White CA, Sparks RB, Erwin WD, Podoloff DA, Lamonica D, Bartlett NL, Parker JA, Dunn WL, Spies SM, Belanger R, Witzig TE, Leigh BR. Biodistribution and dosimetry results from a phase III prospectively randomized controlled trial of Zevalin radioimmunotherapy for low-grade, follicular, or transformed B-cell non-Hodgkin's lymphoma. Crit Rev Oncol Hematol. 2001; 39:181–94. [PubMed: 11418315]
4. Vose JM. Bexxar: novel radioimmunotherapy for the treatment of low-grade and transformed low-grade non-Hodgkin's lymphoma. Oncologist. 2004; 9:160–72. [PubMed: 15047920]
5. Chinn P, Braslawsky G, White C, Hanna N. Antibody therapy of non-Hodgkin's B-cell lymphoma. Cancer Immunol Immunother. 2003; 52:257–280. [PubMed: 12700943]
6. Srivastava S, Dadachova E. Recent Advances in. Radionuclide Therapy. Semin Nucl Med. 2001; 31:330–341. [PubMed: 11710775]
7. Cacheris WP, Nickle SK, Sherry AD. Thermodynamic study of lanthanide complexes of 1,4,7-Triazacyclononane-N,N′,N″-triacetic Acid and 1,4,7,10-tetraazacyclododecane-N,N′,N″,N‴-tetraacetic acid. Inorg Chem. 1987; 26:958–960.
8. Harrison A, Walker CA, Parker D, Jankowski KJ, Cox JP. The in vivo release of ^{90}Y from cyclic and acyclic ligand-antibody conjugates. Nucl Med Biol. 1991; 18:469–476.
9. Hinz FP, Margerum DW. Ligand solvation and the macrocyclic effect. A study of Nickel(II)-Tertramine Complexes. Inorg Chem. 1974; 13:2941.
10. Hancock RD, Martell AE. Ligand design for selective complexation of metal ions in aqueous solution. Chem Rev. 1989; 89:1875–1914.
11. Alvarez RD, Partridge EE, Khazaeli MB, Plott G, Austin M, Kilgore L, Russell CD, Liu T, Grizzle WE, Schlom J, LoBuglio AF, Meredith RF. Intraperitoneal radioimmuno-therapy of ovarian cancer with ^{177}Lu-CC49: a phase I/II study. Gynecol Oncol. 1997; 65:94–101. [PubMed: 9103398]
12. Chappell LL, Ma D, Milenic DE, Garmasteni K, Venditto V, Beitzel MP, Brechbiel MW. Synthesis and evaluation of novel bifunctional chelating agents based on 1,4,7,10-tetraazacyclododecane-*N*,*N*′,*N*′,*N*‴-tetraacetic acid for radiolabeling proteins. Nucl Med Biol. 2003; 30:581–595. [PubMed: 12900284]
13. Stimmel JB, Stockstill ME, Kull FC Jr. Yttrium-90 chelation properties of tetraazatetraacetic acid macroyclices, diethylenetriaminepentaacetic acid analogues, and a novel terpyridine acyclic chelator. Bioconjugate Chem. 1995; 6:219–225.
14. Chakrabarti MC, Le N, Paik CH, De Graff WG, Carrasquillo JA. Prevention of radiolysis of monoclonal antibody during labeling. J Nucl Med. 1996; 37:1384–1388. [PubMed: 8708780]

15. Chong HS, Lim S, Baidoo KE, Milenic DE, Ma X, Jia F, Song HA, Brechbiel MW, Lewis MR. Synthesis and biological evaluation of a novel decadentate ligand DEPA. Bioorg Med Chem Lett. 2008; 18:5792–5795. [PubMed: 18845437]

16. Song HA, Kang CS, Baidoo KE, Milenic DE, Chen Y, Dai A, Brechbiel MW, Chong HS. Efficient Bifunctional Decadentate Ligand 3p-*C*-DEPA for Targeted Alpha Radioimmunotherapy Applications. Bioconjugate Chem. 2011; 22:1128–1135.

17. Chong HS, Garmestani K, Millenic DE, Brechbiel MW. Design, synthesis, and biological evaluation of novel macrocycles with pendant donor groups as radioimmunotherapy (RIT) agents. J Med Chem. 2002; 45:3458–3464. [PubMed: 12139456]

18. Chong HS, Song HA, Kang CS, Le T, Sun X, Dadwal M, Lee HB, Lan X, Chen Y, Dai A. A highly effective bifunctional ligand for radioimmunotherapy of cancer. Chem Commun. 2011; 47:5584–5586.

19. Agus DB, Bunn PA Jr, Franklin W, Garcia M, Ozols RF. HER-2/neu as a therapeutic target in non-small cell lung cancer, prostate cancer, and ovarian cancer. Semin Oncol. 2000; 27:53–63. [PubMed: 11236029]

20. Baselga J. Phase I and II clinical trials of trastuzumab. Ann Oncol. 2001; 12:S49–55. [PubMed: 11521722]

21. Brechbiel MW, Gansow OA. Backbone-substituted DTPA ligands for ^{90}Y radioimmunotherapy. Bioconjugate Chem. 1991:187–94.

22. Camera L, Kinuya S, Garmestani K, Wu C, Brechbiel MW, Pai LH, McMurry TJ, Gansow OA, Pastan I, Paik CH, Carrasquillo JA. Evaluation of the serum stability and in vivo biodistribution of CHX-DTPA and other ligands for yttrium labeling of monoclonal antibodies. J Nucl Med. 1994; 35:882–9. [PubMed: 8176477]

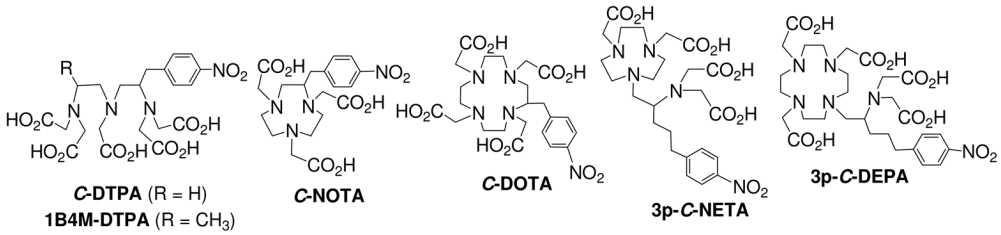

Figure 1.
Bifunctional Ligands in preclinical and clinical evaluation

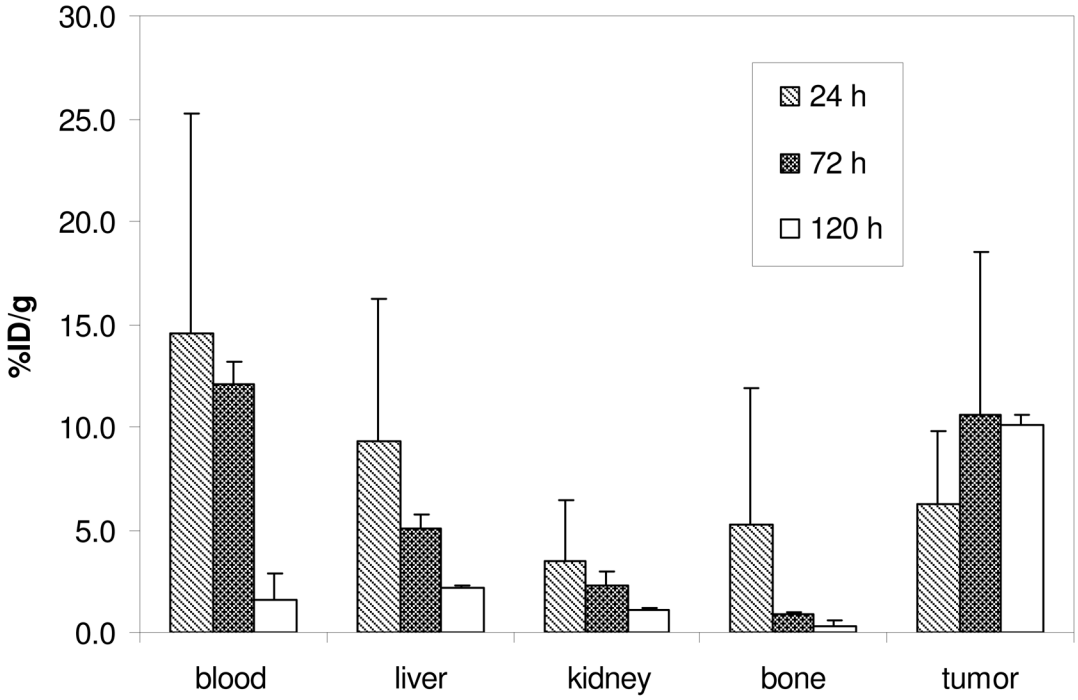

Figure 2.
In vivo biodistribution of ^{177}Lu-3p-*C*-NETA-trastuzumab conjugate in ZR-75-1-bearing mice (% ID/g, n = 3, intravenous injection)

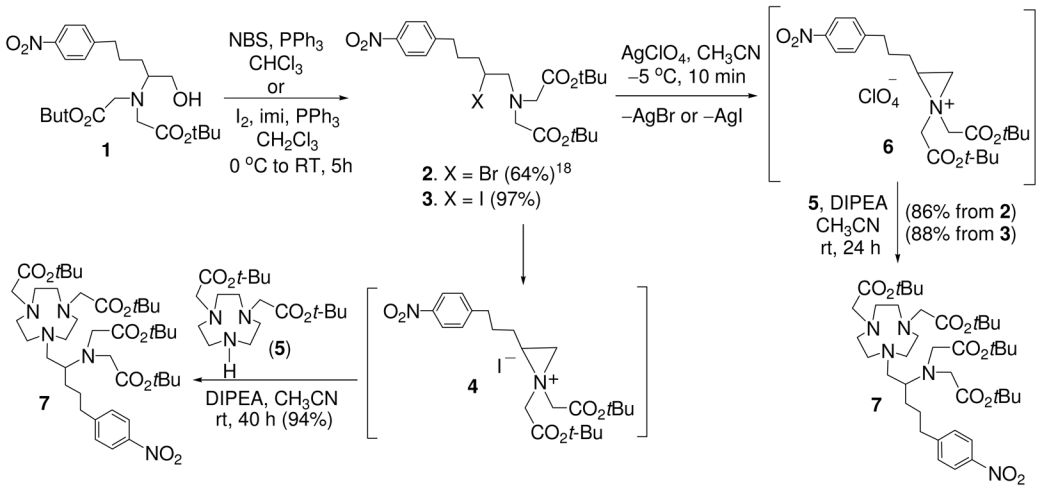

Scheme 1.
Optimized synthesis of the key precursor molecule 7

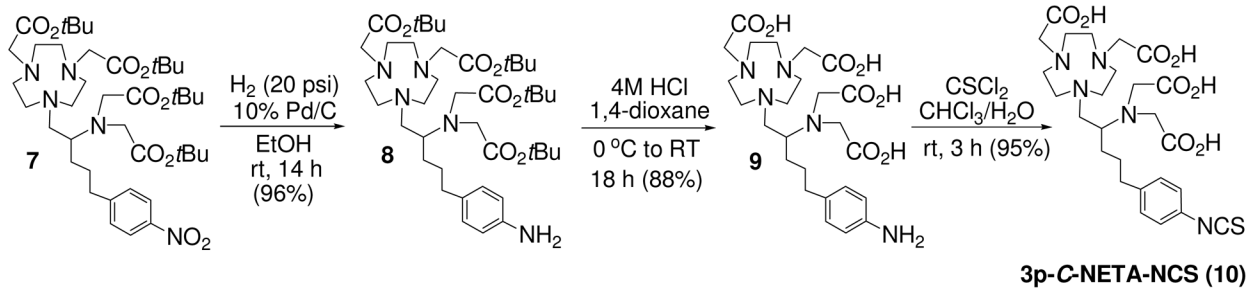

Scheme 2.
Synthesis of bifunctional ligand 3p-*C*-NETA-NCS (10)

Table 1

[a] Evaluation of radiolabling efficiency (%) of bifunctional ligand-trastuzumab conjugates with ^{90}Y (RT, 0.25M NH_4OAC, pH 5.5) using bITLC and cHPLC (parenthesis)

Time	3p-*C*-NETA-trastuzumab	3p-*C*-DEPA-trastuzumab	*C*-DTPA-trastuzumab	*C*-DOTA-trastuzumab
1 min	91.6 ± 3.1 (86.2 ± 3.5)	30.6 ± 1.9 (29.3 ± 2.2)	98.4 ± 0.4 (90.1 ± 1.2)	23.1 ± 7.7 (24.1 ± 6.6)
5 min	99.6 ± 0.2 (94.4 ± 0.2)	58.6 ± 1.6 (50.3 ± 1.8)	98.7 ± 0.7 (89.9 ± 1.3)	43.0 ± 9.9 (39.8 ± 8.3)
10 min	99.6 ± 0.3 (94.9 ± 1.4)	66.3 ± 10.4 (58.2 ± 6.8)	98.6 ± 0.8 (89.5 ± 0.8)	56.5 ± 12.5 (50.9 ± 13.3)
20 min	99.6 ± 0.5 (93.1 ± 1.1)	67.9 ± 7.2 (58.3 ± 7.1)	98.7 ± 0.4 (89.3 ± 0.8)	67.4 ± 12.2 (60.1 ± 15.2)
30 min	99.9 ± 0.1 (93.6 ± 0.9)	67.50 ± 7.5 (57.4 ± 7.3)	98.9 ± 0.3 (90.3 ± 0.6)	69.7 ± 10.8 (62.7 ± 12.4)
60 min	99.8 ± 0.1 (93.4 ± 0.5)	67.4 ± 9.0 (56.9 ± 5.3)	99.2 ± 0.4 (90.0 ± 0.5)	71.7 ± 8.9 (63.4 ± 11.3)

[a] Radiolabeling efficiency (mean ± standard deviation %) was measured in triplicate (n = 3);

[b] ITLC eluent (20mM EDTA/0.15M NH_4OAc);

[c] HPLC mobile phase (0.05M $NaSO_4$/0.02M NaH_2PO_4/0.05% NaN_3, pH 6.8 or PBS, pH 7.4).

Table 2

[a] Evaluation of Radiolabling efficiency (%) of bifunctional ligand-trastuzumab conjugates with ^{177}Lu (RT, 0.25M NH_4OAC, pH 5.5) using bITLC and cHPLC (parenthesis)

Time	3p-*C*-NETA-trastuzumab	3p-*C*-DEPA-trastuzumab	*C*-DTPA-trastuzumab	*C*-DOTA-trastuzumab
1 min	99.2 ± 0.2 (96.5 ± 1.2)	35.9 ± 1.8 (29.8 ± 2.1)	99.5 ± 0.3 (98.3 ± 0.6)	29.7 ± 1.5 (28.1 ± 3.0)
5 min	99.9 ± 0.1 (97.7 ± 0.8)	71.1 ± 2.2 (60.0 ± 1.9)	99.4 ± 0.2 (98.3 ± 0.3)	58.6 ± 1.3 (54.6 ± 1.5)
10 min	99.8 ± 0.1 (97.6 ± 1.3)	85.3 ± 1.1 (75.2 ± 0.4)	99.4 ± 0.4 (98.4 ± 0.7)	75.5 ± 1.7 (70.1 ± 1.6)
20 min	99.9 ± 0.1 (97.6 ± 0.8)	94.8 ± 0.4 (85.4 ± 1.0)	99.6 ± 0.1 (98.3 ± 0.3)	89.3 ± 0.1 (84.6 ± 1.4)
30 min	99.8 ± 0.1 (97.5 ± 0.3)	97.9 ± 0.4 (87.3 ± 1.4)	99.6 ± 0.2 (98.3 ± 0.3)	94.2 ± 0.4 (90.1 ± 1.5)
60 min	99.9 ± 0.1 (97.4 ± 0.4)	98.4 ± 0.8 (87.6 ± 1.3)	99.4 ± 0.3 (98.1 ± 0.3)	97.8 ± 0.3 (94.8 ± 1.3)

[a] Radiolabeling efficiency (mean ± standard deviation %) was measured in triplicate (n = 3);

[b] ITLC Eluent (20mM EDTA/0.15M NH_4OAc);

[c] HPLC mobile phase (0.05M $NaSO_4$/0.02M NaH_2PO_4/0.05% NaN_3, pH 6.8 or PBS, pH 7.4).